



MODELLING OF UNREINFORCED MASONRY INFILL WALLS CONSIDERING IN-PLANE AND OUT-OF-PLANE INTERACTION

S. Kadysiewski¹ and K.M. Mosalam²

¹ Structural Engineer, Bechtel National, Inc., San Francisco, California, skadysie@msn.com

² Professor and Vice Chair, 733 Davis Hall, Department of Civil and Environmental Engineering, University of California, Berkeley, CA 94720-1710, mosalam@ce.berkeley.edu

ABSTRACT

This paper describes a practical analytical model which can be used for the seismic evaluation of unreinforced masonry (URM) infill walls located within a reinforced concrete (RC) frame. The model, consisting of diagonal beam-column members utilizing fiber-element cross sections, is suitable for use in nonlinear time history analyses. The model considers both the in-plane (IP) and the out-of-plane (OOP) responses of the infill, as well as any chosen convex interaction between IP and OOP capacities. The behaviour is elastoplastic, and limit states may be defined by deformations or ductilities in the two directions. These limit states may be chosen to conform to code guidelines or they may be developed independently by the engineer. The model is composed of elements available in commonly used structural analysis software programs. The performance of the model is shown to be satisfactory for static pushover and dynamic analyses using a single panel structure. The proposed infill model is incorporated into a five-storey RC moment frame building with URM infill walls. It is subjected to 20 sets of ground acceleration time histories at five different levels of spectral acceleration. Collapse of the infill panel is assumed to occur at critical displacement ductilities in the IP and OOP directions with interaction between the ductilities considered. Fragility functions, giving the probability of collapse as a function of spectral acceleration level, are calculated and discussed.

KEYWORDS: earthquake, fragility, infill, in-plane, out-of-plane, model.

INTRODUCTION

Reinforced concrete (RC) frames containing unreinforced masonry (URM) infill walls are a commonly used structural system, both in North America and around the world. It is recognized that many buildings of this type have performed poorly during earthquakes. The 2008 Wenchuan earthquake in China provides numerous examples of frame-wall interaction (Figure 1).



Figure 1: Infill damage after the 2008 Wenchuan, China earthquake [1]

It is a common practice to analyze RC frames containing URM infill walls as concentric braced frames, with the diagonal elements of the model representing the infill wall. Such models are computationally efficient, relative to the alternate method of modelling the infill panels with finite element (FE) methods. In most procedures, e.g. FEMA 356 [2], the analysis model includes the in-plane (IP) behaviour only. Out-of-plane (OOP) behaviour is considered independently, with no interaction considered between IP and OOP behaviour. However, work by Hashemi and Mosalam [3] has indicated that such interaction may be significant in calculating the seismic vulnerability of such structural systems. This paper proposes a practical analytical model, Figure 2, which can include the effects of both IP and OOP strengths and the interaction between them. Such a model is intended for use in nonlinear time history analyses. For each infill panel, representing a single bay in a single storey, the model consists of one diagonal member. That member is composed of two beam-column elements, joined at the midpoint node, which is given a lumped mass in the OOP direction. The surrounding frame elements (dashed lines in Figure 2) are not part of the proposed infill panel model, and are shown in Figure 2 for reference only. Such elements are handled separately using well-known modeling techniques of framed structures. The infill model takes advantage of the ability, e.g. using OpenSees [4], to model a cross-section as an arbitrary collection of nonlinear fiber elements. The procedure for constructing this model is discussed in the following sections.

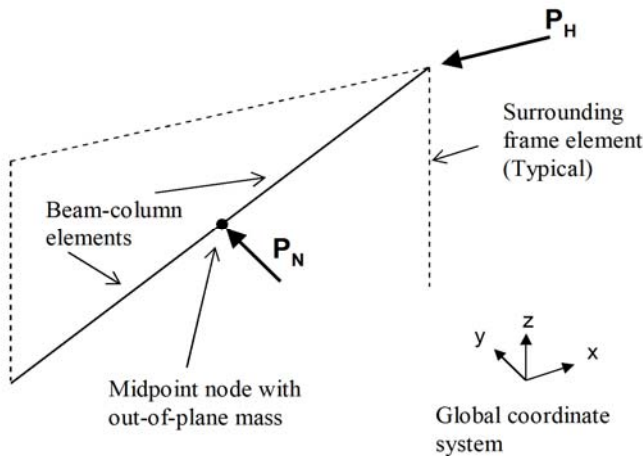


Figure 2: Proposed infill wall model using beam-column elements with fiber discretization

It should be pointed out that the formulation of the proposed model is different from that used by FEMA 356 [2], in that it uses only one diagonal member rather than the two compression-only diagonal struts used in [2]. This is because, as will be seen later, using only one diagonal member is sufficient to satisfy the IP–OOP interaction relationship. Therefore, the proposed model uses a diagonal member with both tension and compression strengths. This single diagonal member approach causes a somewhat different distribution of forces in the surrounding structure. However, if the floor diaphragms are relatively stiff and strong, as is often the case, the consequences of this simplification are expected to be minor.

It is desirable for the fiber section model to exhibit the following attributes, relative to the actual infill wall that it represents:

- 1) For pure IP behaviour, the model should provide a prescribed axial stiffness and strength.
- 2) For OOP deflections, the model should have the same natural frequency as the infill wall. It should produce the same OOP support reactions as the actual infill wall. Moreover, it should exhibit initial yielding in the OOP direction at the same level of support motion that causes the infill wall to yield.
- 3) For combined IP and OOP behaviour, the model should exhibit the specified strength interaction (discussed later) between IP strength and OOP strength.
- 4) For simplicity, in the post-yield region the model is designed to behave in a perfectly plastic manner, i.e. there is no degradation of the stress in the model materials with increasing strain.

PROPERTIES OF THE INFILL PANEL

Calculations for the elastic stiffnesses and unidirectional strengths of the infill panel are based on FEMA 356 [2]. These procedures are well known, and will not be repeated here, refer to [5] for details. The strength interaction curve is taken as a 3/2–power curve,

$$\left(\frac{P_N}{P_{N0}}\right)^{\frac{3}{2}} + \left(\frac{P_H}{P_{H0}}\right)^{\frac{3}{2}} \leq 1.0 \quad (1)$$

where P_N is the OOP capacity in the presence of IP force, P_{N0} is the OOP capacity without IP force, P_H is the IP capacity in the presence of OOP force, and P_{H0} is the IP capacity without OOP force. The proposed relationship in Equation 1 is compared in Figure 3 with the FE results reported in [3].

PROPERTIES OF THE FIBER CROSS SECTION

The IP–OOP relationship given in Figure 3 is based upon IP and OOP forces. However, since the diagonal member of the infill model is pin-connected to the surrounding structure, it is possible to express the relationship as a P – M relationship at the middle node of the diagonal, where P is the axial force in the diagonal and M is the OOP bending moment. The arrangement of nonlinear fibers at the midspan is shown in Figure 4a, and the discretization of the interaction relationship is shown schematically in Figure 4b.

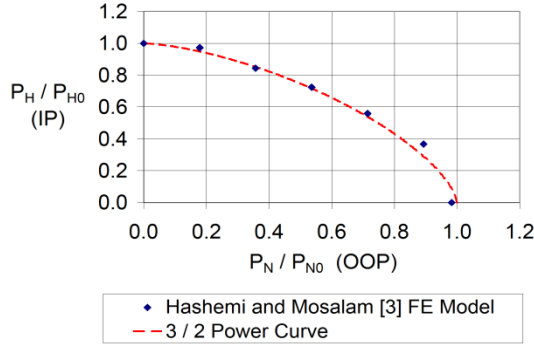


Figure 3: Interaction curve for IP and OOP strengths

In order to derive the equations for the strength and the location of the fibers, it is useful to consider the changes in the resultant axial force, P , and bending moment, M , at the midspan hinge as the plastic neutral axis (PNA) is “swept” through the cross section, successively occupying positions between each of the fibers. Referring to Figure 4a, all of the fibers are on one side of the PNA when it is at the location designated “PNA 1,” and hence all fiber forces have the same sign (assume compression to start). This produces pure compression, corresponding to the point “ $j=1$ ” on the $P-M$ diagram (Figure 4b). Next, the PNA is moved to position “PNA 2.” Since fiber 1 (the outermost fiber) changes from compression to tension, the axial force in the cross section decreases by an amount $2F_{y1}$, where F_{y1} is the yield force of fiber 1. Also, the bending moment in the cross section increases by an amount $2F_{y1}z_1$, since fiber 1 and its corresponding fiber on the opposite side of the cross section form a tension-compression couple. Here z_1 is the distance from the y -axis to fiber 1. These changes in axial force and bending moment can be set equal to the corresponding changes in the first segment of the $P-M$ diagram, giving

$$F_{y1} = \frac{1}{2}[P_1 - P_2] \quad \text{and} \quad z_1 = \frac{1}{2} \left[\frac{M_2 - M_1}{F_{y1}} \right] \text{ with } M_1 = 0 \quad (2)$$

Using the indicated choice of indices, where the fiber farthest from the centroid, and the point of pure compression on the $P-M$ diagram, are each given the index “1” with $i=j$ in Figure 4, we can write the general equations for the strength and locations of the fibers as

$$F_{yi} = \frac{1}{2}[P_i - P_{i+1}] \quad \text{and} \quad z_i = \frac{1}{2} \left[\frac{M_{i+1} - M_i}{F_{yi}} \right] = \left[\frac{M_{i+1} - M_i}{P_i - P_{i+1}} \right] \quad (3)$$

The strength and stiffness properties of the fibers are calculated sequentially, starting from the outside, and progressing inward to the y -axis. Note that there are as many fibers on each side of the y -axis as there are segments in the $P-M$ diagram. Since the fibers are assumed to be symmetric about the y -axis, with equal tensile and compressive strengths, the full interaction curve for the fiber-element cross section is symmetric about both the P -axis and the M -axis (see Figure 5a, where P and M are normalized by their unidirectional capacity). Relaxation of these conditions would allow modelling of non-symmetric interaction relationships.

Note: fiber areas and locations are symmetric with respect to the y-axis

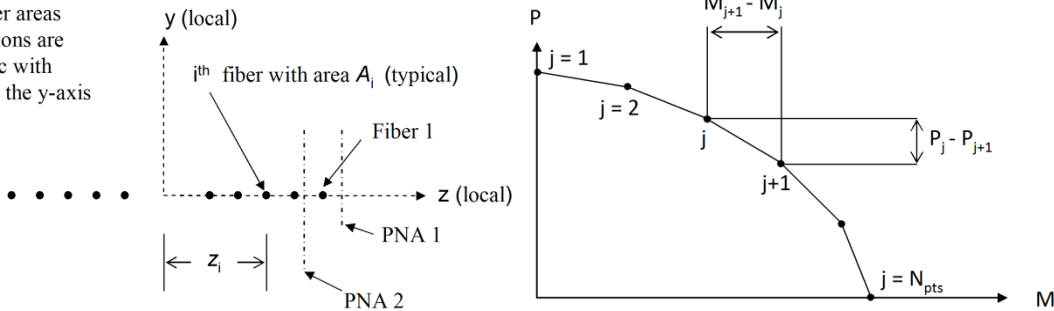


Figure 4: Fiber element model: a) Fiber layout; b) Discretized P-M interaction curve

Referring to the last of Equations 3, it is noted that the i^{th} fiber location is equal to the negative inverse of the slope of the i^{th} segment of the P - M diagram, since each fiber element corresponds to a segment of the P - M curve. For a concave interaction diagram, defined here as one in which the $(i+1)^{\text{th}}$ segment has a slope smaller (in algebraic sense) than that of the i^{th} segment, the calculated z_{i+1} will be greater than z_i . Since this violates the assumption made in the derivation, i.e. that the calculations in Equation 3 proceed from the outside to the inside of the cross section, it is not possible to model concave interaction diagrams using this method. This limitation is not considered to be serious, however, since such an interaction diagram is rarely encountered. For calculations regarding the fiber elastic properties, the reader is referred to [5] for complete details and numerical examples.

FAILURE CRITERIA FOR THE PROPOSED INFILL MODEL

FEMA 356 [2] gives criteria for “failure” of the infill panels, taken in this paper as the “collapse prevention” (CP) level. These criteria are based on the IP and OOP deformation of the infill panel, and are given for unidirectional deformations only. Since the exact nature of the interaction between IP and OOP collapse deformations awaits further research, it is decided, for convenience, to also use a 3/2-power relationship. It should be noted that the CP criteria are not part of the behaviour of the model, i.e. the model strengths do not drop to zero when the CP interaction line is crossed. The consequences of (and possible remedies for) this limitation are discussed later. The P - M and displacement interaction relationships are shown in Figure 5. Note that Δ_H is the IP horizontal displacement, Δ_N is the OOP horizontal displacement, and Δ_{Hy0} and Δ_{Ny0} are their respective “yield” (strength divided by elastic stiffness) values, assuming zero displacement in the other direction.

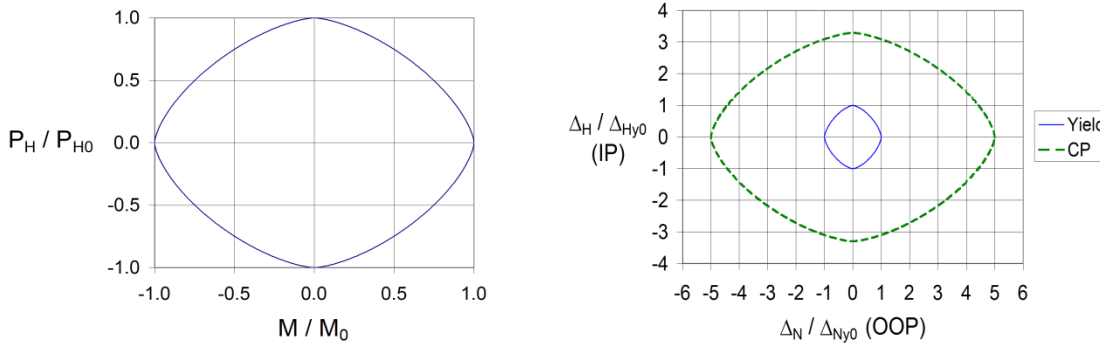


Figure 5: Interaction Relationships: a) P-M; b) deformation criteria

PERFORMANCE OF THE PROPOSED INFILL MODEL

In order to verify the performance of the proposed fiber cross section of diagonal member representing an infill wall, a single bay, single storey model (Figure 2) is created using OpenSees [4]. Nonlinear behaviour is obtained by placing a nonlinear fiber cross section, as described above, at the midspan of the diagonal. First, the model is analyzed for static pushover, applying a fixed static force, P_N , in the OOP direction, then performing a displacement-controlled pushover analysis in the IP direction. An example of this type of analysis is given in Figures 6 and 7. For the shown case, an OOP static force of 13.3 kN (3 kips), representing 46% of P_{N0} , is applied to the model, which is then pushed in the IP direction under IP displacement control. Figure 6 shows the resulting pushover curve, i.e. the IP shear force versus the IP horizontal displacement. Figure 7a shows the corresponding path on the $P-M$ diagram. Note that the path does not exceed the prescribed interaction boundary. This is a consequence of the methodology of choosing the strength of the cross-section fibers derived above. Finally, Figure 7b shows the path of the displacements, normalized by the respective unidirectional yield displacements. As clearly observed, the shape of the displacement path is similar to that of the $P-M$ path while the fibers are elastic; after crossing the yield surface the path bends more sharply. For the case shown, the displacement path also crosses the outer interaction surface, indicating that the infill wall has exceeded the CP limit state. Examples of cyclic pushover and dynamic behaviour of the proposed model are given in [5].

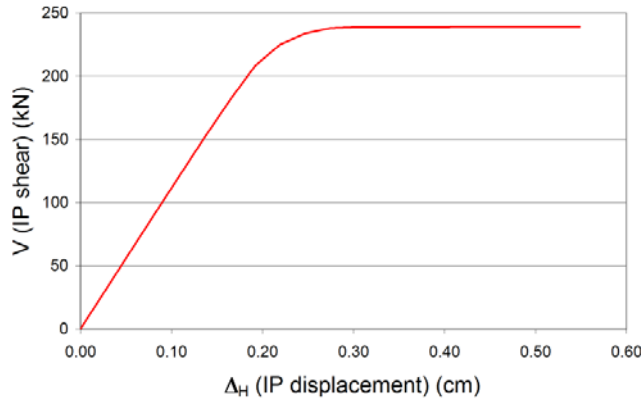


Figure 6: In-plane pushover curve with $P_N = 46\%P_{N0}$

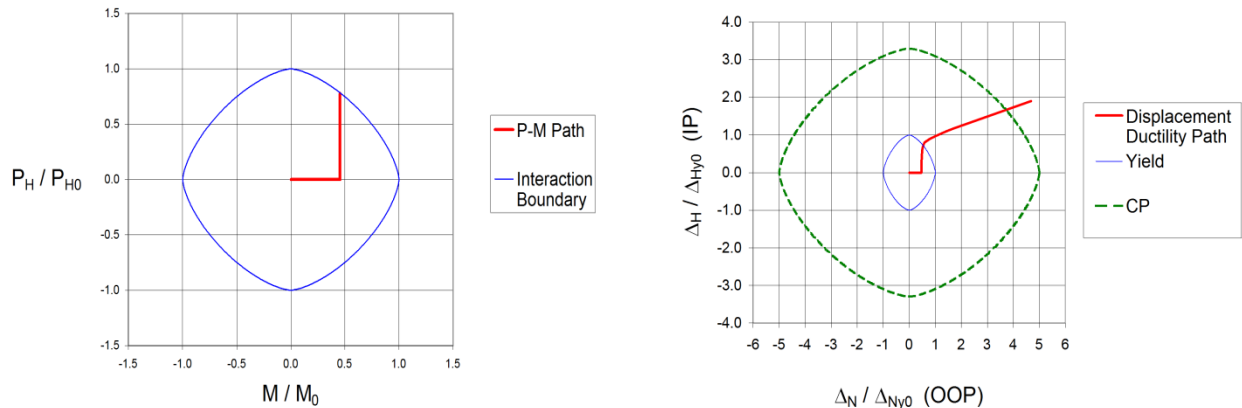


Figure 7: Pushover path with $P_N = 46\%P_{N0}$: a) P-M path; b) Deformation path

EXAMPLE ANALYSIS OF A 5-STORY BUILDING

In order to demonstrate the behaviour and capabilities of the developed infill model, the model is incorporated into a larger OpenSees [4] model of a 5-storey RC frame building with URM infill walls where bay spans are 4114 mm (13.5 ft) in the longitudinal direction (parallel to the URM wall) and 3658 mm (12 ft) in the transverse direction; storey heights are 3658 mm (12 ft); URM infill walls are 104 mm (4 in) thick; material properties are based on the actual tested values in [3] with masonry prism compression strength is 17.0 MPa (2.46 ksi). The model, shown in Figure 8a, is based on previous work by Hashemi and Mosalam [3], where full details are given. It consists of RC beams and columns, tied together by RC diaphragms (not shown) at the floor levels. The URM infill is located along the center frame on Line B, where the developed infill model is applied in all bays of each storey (see Figure 8b). The model is subjected to seismic base excitation, using 20 sets of ground motion (see Lee and Mosalam [6]), each set consisting of longitudinal and transverse components. These motions are scaled such that their spectral accelerations, S_a , at the fundamental periods in each direction of the building model are set to five values: 0.50g, 1.00g, 1.61g, 2.05g, and 2.75g [3].

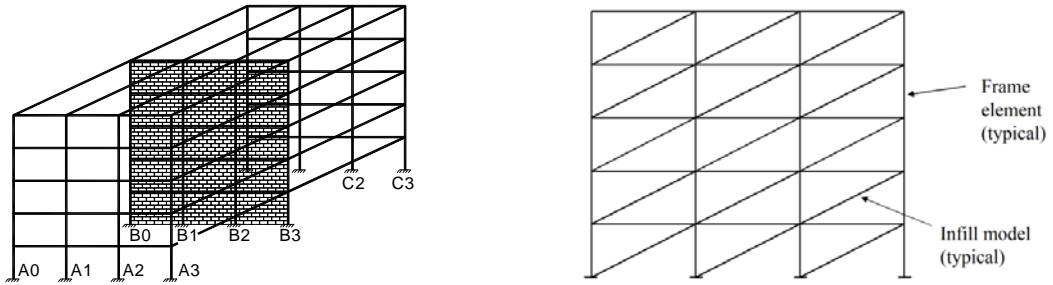


Figure 8: 5-Storey building model: a) Isometric view; b) Elevation of Line B with infills

As an example, the response of the model to the motion recorded at the Gilroy #6 station during the 1979 Coyote Lake earthquake, scaled such that $S_a = 1.0\text{g}$, is shown in Figures 9 and 10. Figure 9 shows the IP and OOP displacements of the center bay of the first storey. Figure 10 shows the $P-M$ and deformation paths in their respective planes. It is noted that the permanent, residual inelastic displacement is more prominent for the OOP direction than the IP direction, despite the fact that the force-moment path touches the yield surface near the pure axial force vertex. This is because there is significant IP structural redundancy provided by the RC moment frame (which is seismically designed [3]), preventing the IP displacements from increasing rapidly after yield. In the OOP direction, however, there is no redundancy, and this permits the OOP displacements to grow rapidly. Note that the CP limit state interaction function is exceeded.

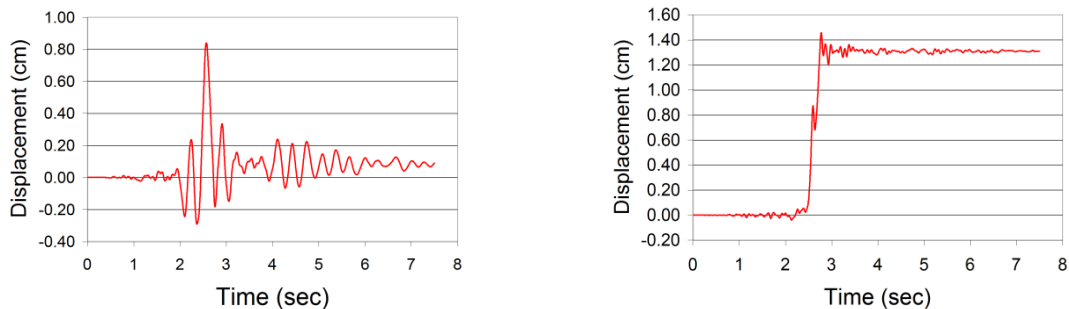


Figure 9: Displacement time histories: a) in-plane; b) out-of plane

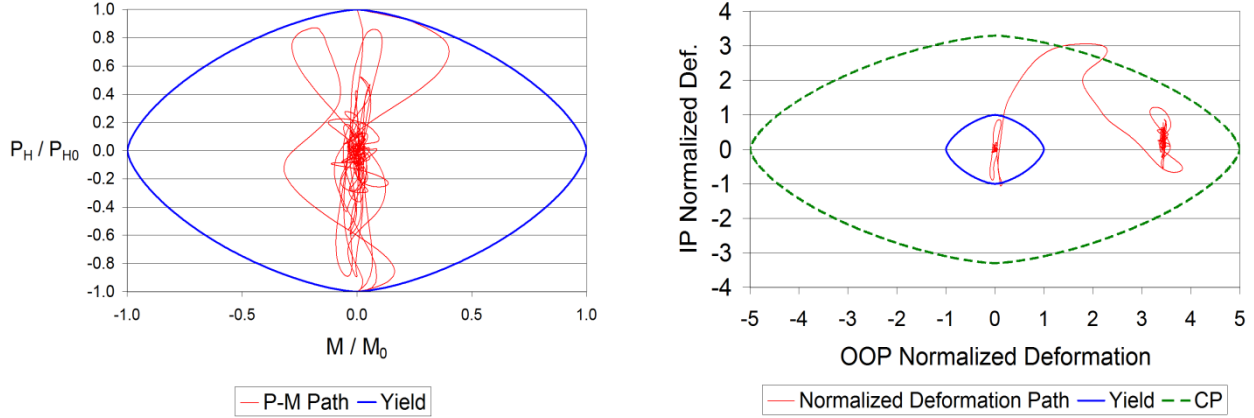


Figure 10: Interaction paths: a) P-M; b) deformation

FRAGILITY CURVES FOR THE INFILL PANELS

It is possible to construct fragility curves, given the results of the 100 time history analyses (20 time histories at 5 levels of S_a) discussed in the previous section. Here, a fragility curve or function is defined as the probability that the response of a particular infill panel will exceed a chosen limit state, for a given spectral acceleration S_a . Collapse prevention (CP), as defined above, is the chosen limit state (LS). It is assumed at this stage that only record-to-record variability affects the resulting probabilities. In order to facilitate calculations, define a variable known as the deformation interaction ratio (DIR) as follows:

$$DIR(t) = \left[\left(\frac{\Delta_H(t)}{\Delta_{Hcp0}} \right)^{\frac{3}{2}} + \left(\frac{\Delta_N(t)}{\Delta_{Ncp0}} \right)^{\frac{3}{2}} \right]^{\frac{2}{3}} \quad (4)$$

where Δ_{Hcp0} and Δ_{Ncp0} are analogous to Δ_{Hy0} and Δ_{Ny0} , respectively, but for the CP limit state. This definition is derived from the 3/2-power interaction curves discussed earlier. The CP limit state is reached when $DIR = 1.0$. The 2/3 exponent is added for geometrical clarity. It permits the DIR to be estimated visually from a normalized deformation path such as Figure 10b. The calculations for the fragility functions in this study proceed as follows:

- 1) At each S_a level, the maximum DIR is determined for each earthquake record. The distribution of the DIR 's is assumed to be lognormal.
- 2) The mean and sample standard deviation are found for the $\ln DIR$'s for each set of the 20 records. Note that the infill panel reaches the CP limit state when $\ln DIR = 0.0$.
- 3) Finally, the probability of reaching or exceeding the CP limit state is given by:

$$P(LS \geq CP) = 1 - Pr_{norm}(0, \mu_{\ln DIR}, \sigma_{\ln DIR}) \quad (5)$$

where $\mu_{\ln DIR}$ and $\sigma_{\ln DIR}$ are respectively mean and sample standard deviation of the $\ln DIR$'s from the 20 records, and $Pr_{norm}(0, \mu_{\ln DIR}, \sigma_{\ln DIR})$ = cumulative probability that the normal random variable $\ln DIR$ will exceed 0.0, given $\mu_{\ln DIR}$ and $\sigma_{\ln DIR}$.

The procedure described above is performed for each of the five selected levels of S_a . As an example, the fragility function for the infill panel of the first storey, center bay, is given in Figure 11. As shown in this example, there is approximately a 50% probability of exceeding the CP limit state for an earthquake with $S_a = 1.0\text{g}$, while at $S_a = 2.5\text{g}$ the probability of exceedence is greater than 95%. It is possible to obtain a measure of the IP-OOP interaction effects by examining DIR 's for the IP and OOP deformations separately. Define

$$DIR_IP(t) = \frac{\Delta_H(t)}{\Delta_{Hcp0}} \quad \text{and} \quad DIR_OOP(t) = \frac{\Delta_N(t)}{\Delta_{Ncp0}} \quad (6)$$

Fragility curves may be calculated for these DIR 's, as shown in Figure 11. It is clear from this figure that the probability of reaching the CP limit state is higher when interaction effects are considered, than for the case where interaction is ignored. Whether these differences would have significant impacts on project decisions can only be determined on a case-by-case basis, but the nontrivial magnitudes of the differences indicate that some consideration should be given for this interaction effect, at least in an informal way.

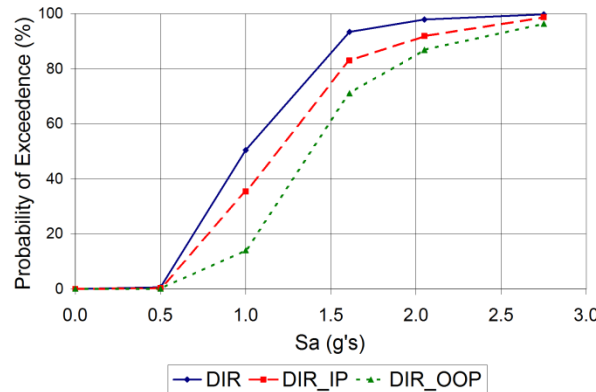


Figure 11: Combined, IP, and OOP CP fragility functions for the first storey, center bay, infill panel

The vulnerability functions discussed above have been calculated considering only the effects of record-to-record variability. The effect of, e.g. masonry strength, on the vulnerability functions has also been studied [5] using a first-order, second-moment (FOSM) analysis, and found to be relatively minor.

CONCLUSIONS AND RECOMMENDATIONS

The following is a list of conclusions and recommendations that can be inferred from the study presented in this paper:

- 1) The simple infill model described in this paper generally meets the goals stated for its development. It reproduces the elastic stiffness of the infill and the reaction forces on the surrounding structure. The strength properties of the infill, both in the IP and the OOP directions, and the interaction between them, are accurately captured. In the inelastic range, however, the model behaviour requires further development. It is not possible, using elastic, perfectly plastic (EPP) fibers, to fully control the inelastic behaviour. Modifying the post-yield properties of the fibers may improve the situation, at a cost of added complexity.

- 2) Another more serious objection stems from the fact that the model IP axial and OOP bending moment strengths do not drop to zero when the CP limit state interaction curve is exceeded. In the actual structure, the collapse of an element is accompanied by an increase of load in neighboring elements. This effect will not be captured with the proposed model, where the collapse of the element, i.e. reaching the CP limit, is determined in post-processing of the analysis results. This may not be a problem if the design engineer intends to redesign or retrofit the walls where collapse is predicted, thus preserving their ability to carry load. However, if the objective of the analysis is a performance-based evaluation of an existing structure, use of the proposed model may lead to unrealistically optimistic conclusions. One crude yet conservative remedy for this problem is to simply remove the “collapsed” infill panel elements, rerun the analysis, and repeat this process until no more panels collapse, or until there is a global collapse of the structure. A more realistic, although more difficult, solution would be to modify the analysis program such that it directly removes the collapsed elements, when they collapse, and then proceeds with the analysis without interruption. This method of direct element removal has been proposed and utilized by Talaat and Mosalam [7].
- 3) Interaction between the IP and OOP strengths of the infill has a measurable effect on vulnerabilities, and may need to be considered in structural engineering practice.

ACKNOWLEDGEMENTS

The authors would like to express their appreciation to Dr. Alidad Hashemi, for generously sharing both his advice and his OpenSees models.

REFERENCES

1. Li, B., Wang, Z., Mosalam, K. M., and Xie, H. (2008), “Wenchuan Earthquake Field Reconnaissance on Reinforced Concrete Framed Buildings With and Without Masonry Infill Walls”, *The 14th World Conference on Earthquake Engineering*, Beijing, China.
2. Federal Emergency Management Agency (FEMA) (2000), “Prestandard and Commentary for the Seismic Rehabilitation of Buildings”, FEMA 356, Washington, D.C.
3. Hashemi, S.A. and Mosalam, K.M. (2007), “Seismic Evaluation of Reinforced Concrete Buildings Including Effects of Infill Masonry Walls”, Pacific Earthquake Engineering Research Center, PEER 2007/100.
4. Mazzoni, S., McKenna, F., Scott, M.H., and Fenves, G.L. (2006), “Open System for Earthquake Engineering Simulation (OpenSees), User Command-Language Manual”, Pacific Earthquake Engineering Research Center, <http://opensees.berkeley.edu/OpenSees/manuals/>.
5. Kadysiewski, S. and Mosalam, K.M. (2009), “Modeling of Unreinforced Masonry Infill Walls Considering In-Plane and Out-of-Plane Interaction”, Pacific Earthquake Engineering Research Center, PEER 2008/102.
6. Lee, T.-H. and Mosalam, K.M. (2006), “Probabilistic Seismic Evaluation of Reinforced Concrete Structural Components and Systems”, Pacific Earthquake Engineering Research Center, 2006/04.
7. Talaat, M. M. and Mosalam, K.M. (2008), “Computational Modeling of Progressive Collapse in Reinforced Concrete Frame Structures”, Pacific Earthquake Engineering Research Center, PEER 2007/10.